CARBON 2019
LEXINGTON, KY

HIERARCHICALLY POROUS CARBONS WITH SIMULTANEOUSLY HIGH SURFACE AREA AND COLOSSAL PORE VOLUME VIA ICE TEMPLATING

Luis Estevez[1*], Adam L. Garcia[2], Venkateshkumar Prabhakaran[2], Yongsoon Shin[2], Jinhui Tao[2], Dushyant Barpaga[2], Radha K. Motkuri[2], Jitendra Kumar[1]

[1]*Univeristy of Dayton Research Institute, Dayton, OH, USA*
[2]*Pacific Northwest National laboratory, Richland, WA, USA*

*Presenting author's e-mail: Luis.Estevez@UDRI.Udayton.edu

Introduction

Hierarchical porous carbon (HPC) materials have garnered much interest recently[1-3], as the specific ability to utilize a multi-modal pore size distribution across multiple length scales has been shown to be useful. The inherent characteristics of carbon (relatively inert, good electrical conductivity and low density) combines well with a tunable hierarchal porosity in various applications, though the advantages of multimodal pore sizes in HPC materials differ depending on the application(s) for which they are utilized. Recently, Sahore *et al.*[4] have demonstrated that for higher loadings of Li-S composite cathodes (~80% sulfur), combinations of high surface areas along with large pore volume values are both important. Unfortunately, having both high surface area and large pore volume in one material requires a well-controlled HPC morphology and is very difficult to achieve. This is because high surface areas (>1500 m^2/g) are usually associated with smaller pores (<5 nm), whereas large pore volume values (>3 cm^3/g) require larger sized pores—typically at least tens of nanometers.

Herein, we report a rational approach for synthesizing a graphitic HPC system (labeled as HPC-G) and utilizing it as a tunable materials platform with exquisite morphological control of the HPC that enables the realization of extremely high surface area (>2900 m^2/g) and colossally large pore volume (>11 cm^3/g) values. We also show how we utilized ice templating to synergistically achieve these unique textural characteristics. For comparison of the graphitic structure in the HPC-G materials platform, a hard carbon (more atomically disordered) material was also synthesized with similar textural properties to the HPC-G materials and denoted as HPC-S.

Materials and Methods

Synthesis for the HPC-S materials follows procedures outlined in previous work[5]. Briefly, in a typical synthesis process for the hard carbon HPC-S material, a 15 wt.% aqueous suspension of 4 nm colloidal silica (Alfa Aesar) was mixed under medium stirring with sucrose (the ratio of silica to sucrose is 2:1 by wt.). After combining the components together into a homogeneous dispersion, the mixture was poured into an aluminum mold. The mold was thereafter placed into an open container, whereupon liquid nitrogen was poured into the container until the liquid nitrogen level was just below the top of the mold, ice templating the mixture. After the mixture was completely frozen, the mold was moved into a lyophilizer (Labconco 74000 series) for freeze drying. After the water was completely removed via sublimation, the resultant material was then placed into a tube furnace (MTI GSL-1700-X) where it underwent pyrolysis under an argon environment, reaching a target temperature of 1000°C at a ramp rate of 3°C/min. The sample was held at 1000°C for 3 hours and afterwards cooled to room temperature at a rate of 3°C/min. Next, the sample was

placed in 3M NaOH under medium stirring at 80°C, overnight to remove the silica hard template, forming the mesopores. After etching the silica, the porous carbon was washed with DI water until a pH of 7 was reached, whereupon the sample was dried in a vacuum oven at 80°C overnight. The final product was an HPC material with macropores from the ice templating and mesopores from the silica hard template designated as HPC-S-w-xy; where the S represents the sucrose precursor, the w represents the colloidal silica size (in nm) and the xy represents the ratio of silica to the precursor at x:y. For the physical activation process, the HPC-S sample was placed into a tube furnace and ramped up to 900°C at a rate of 5°C/min under argon. Once at 900°C, CO_2 gas was introduced at a flow rate of 50 cm^3/min for a selected time, in hours. The activated sample is designated as HPC-S-w-xy-zh, where z is indicative of the hours that the HPC sample underwent activation. The –zh portion of the sample name is left off for samples that have not undergone activation. The synthesis for the graphitic HPC-G family of porous carbons was similar except for the use of polyacrylonitrile in dimethyl sulfoxide instead of sucrose in water. The freeze dried HPC-G material also underwent an oxidative stabilization step (280°C, 1h) and was pyrolyzed to 1000°C and the silica template removed as before (for the HPC-S), but afterwards, the sample was pyrolyzed further to a higher (1600°C) final temperature.

Results and Discussion

Though the macroporosity created via ice templating is easily tunable[6,7] and we have shown in previous work[5] that the mesoporous pore size distribution (PSD) is also adjustable, we concentrated on utilizing activation to increase the already high surface area and pore volume of our HPC-G materials. We employed a 12 nm colloidal silica template at a silica-to-PAN mass ratio of 2:1, resulting in the HPC-G-12-21 sample. The HPC-G-12-21 samples underwent physical activatvation[8] resulting in extremely high textural properties of both specific surface area (2933 m^2/g) and pore volume (11.23 cm^3/g) together in one material.

Scanning electron microscopy or SEM (**Figure 1a**), reveals the typical macroporous structure present in the HPC-G materials platform. Transmission electron microscopy (TEM) images (**Figure 1b**) of the HPC-G-12-21 sample show a mesoporous PSD distribution centered at ~15 nm, consistent with the colloidal silica particle size. More significantly, the high resolution TEM (HRTEM) images confirm the presence of a graphitic structure. **Figure 1c** shows a typical higher magnification HRTEM image of the individual mesopores for the HPC-G material. The image reveals the mesopore walls are made up of layers of graphitic sheets spaced ~0.34 nm apart (**Figure 1d**), consistent with a more ordered, graphitic structure. The TEM images for the heavily activated HPC-G-12-21-5h carbon (**Figure 1e-f**) reveal the mesoporous PSD broadens out to ~20 nm, in good agreement with the nitrogen porosimetry data (*vide infra*); while the HRTEM image (**Figure 1f**), also shows a well ordered and graphitic structure—albeit with thinner mesoporous walls when compared to the unactivated HPC-G-12-21 carbon. This graphitic structure for the HPC-G materials is noteworthy particularly when combined with the textural properties for the activated HPC-G-12-21 materials (**Table 1**). Such high surface areas are rare for porous graphitic carbons; with most cases in the literature being below 2000 m^2/g.[9-11]

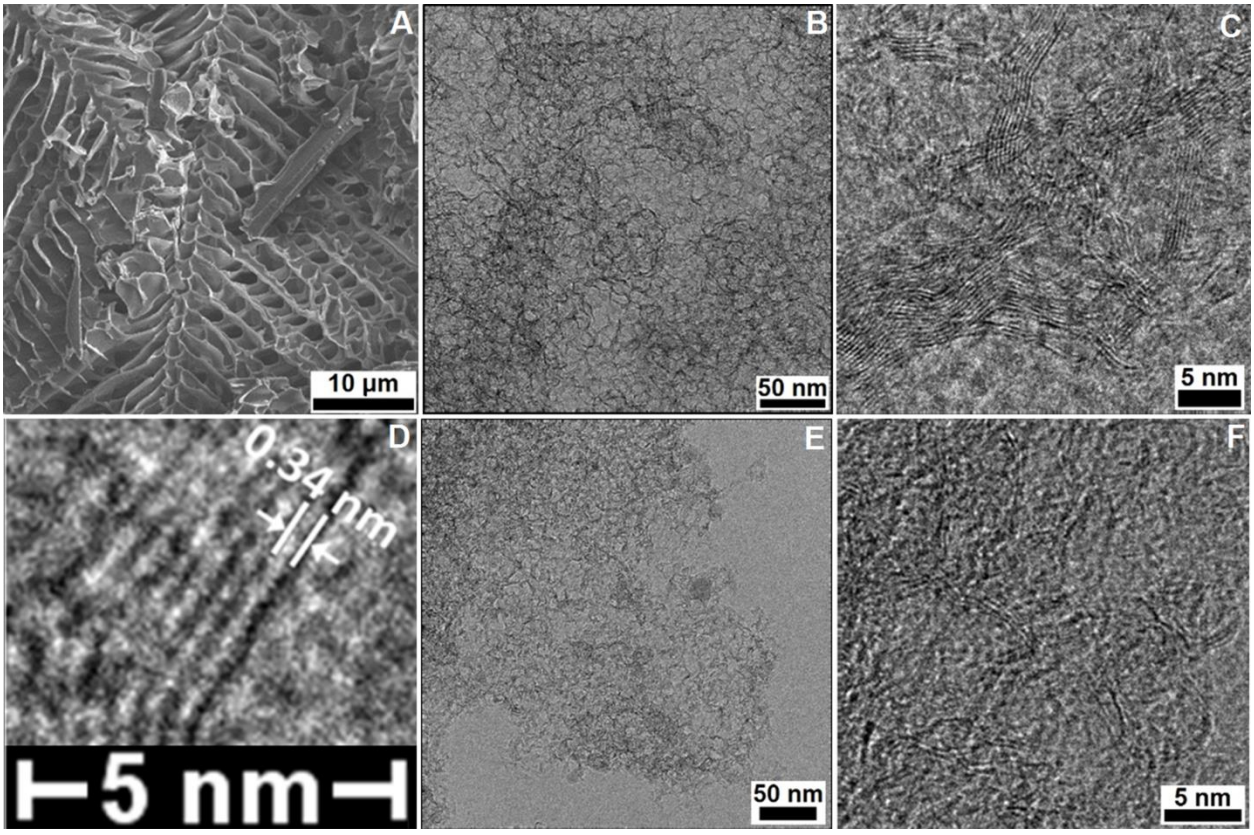

Figure 1. Results of electron microscopy for the HPC-G-12-21 sample reveals (a) the macroporous structure as seen by SEM and the (b) mesopores present in the macroporous walls under TEM, as well as (c,d) the graphitic ordering under HRTEM. The heavily activated HPC-G-12-21-5h sample shows (e) similar mesopores present under TEM and (f) graphitic ordering via HRTEM.

Table 1. Textural characteristics, level of graphitization and oil sorption data for various porous carbons

Porous carbon	BET SSA [m^2/g]	Micropore SSA [m2/g][a]	Total pore volume [cm3/g][b]	Micropore volume [cm3/g][a]	Mesopore volume [cm3/g][c]
HPC-G-1000C	652	83	2.01	0.042	1.49
HPC-G-12-21	619	74	2.47	0.035	1.70
HPC-G-12-21-3h	1831	259	7.03	0.131	4.85
HPC-G-12-21-5h	2933	488	11.51	0.247	7.53
HPC-S-4-21	1292	187	4.89	0.098	4.40
HPC-S-4-21-10h	2675	465	10.84	0.242	7.91
Norit AC	1948	389	1.14	0.209	0.61
KB-600JD	1477	43	4.75	0.014	2.24

[a] Microporous surface area determined via the t-plot method, [b] total pore volume obtained via nitrogen uptake at the single point P/Po value of ~0.995 and [c] mesopore volume was calculated by selecting the BJH cumulative pore volume value at a pore size of 50 nm and subtracting the t-plot micropore volume.

Nitrogen porosimetry was also used to better elucidate the morphology present in the HPC-G-12-21 samples during various stages of synthesis. **Figure 2** shows the nitrogen porosimetry data for the HPC-G-12-21 samples before high temperature pyrolysis (HPC-G-1000C) and after the ensuing high temperature pyrolysis (HPC-G-12-21), as well as after later increasing levels of activation. As can be seen in **Figure 2a**, the HPC-G-1000C sample's PSD (by volume) reveals

mesopores centered at ~15 nm. After pyrolysis at 1600°C, the PSD broadens slightly to larger mesopores, increasing the mesopore volume. Furthermore, there is a smaller 2-3 nm peak also present in the PSD (**Figure 2a-b**) in addition to the 15 nm peak. Upon activation of the HPC-G-12-21 sample, that smaller 2-3 nm peak becomes more prominent, while another peak centered at ~8 nm emerges from the shoulder of the unactivated HPC-G-12-21 sample. There are also micropores that contribute to the higher SSA values that, while beyond the limit of the Barrett-Joyner-Halanda (BJH) analysis, can be measured by way of the calculated t-plot micropore surface area. **Figure 2c** reveals that roughly 82% (9.21 cm^3/g) of the pore volume is from pores ≤100 nm and roughly 70% of the pore volume arises from pores sized ≤50 nm (~7.78 cm^3/g). Removing the pore volume calculated via the t-plot analysis indicates that the mesopore volume is 7.53 cm^3/g—extremely high, especially considering the graphitic nature of the material.

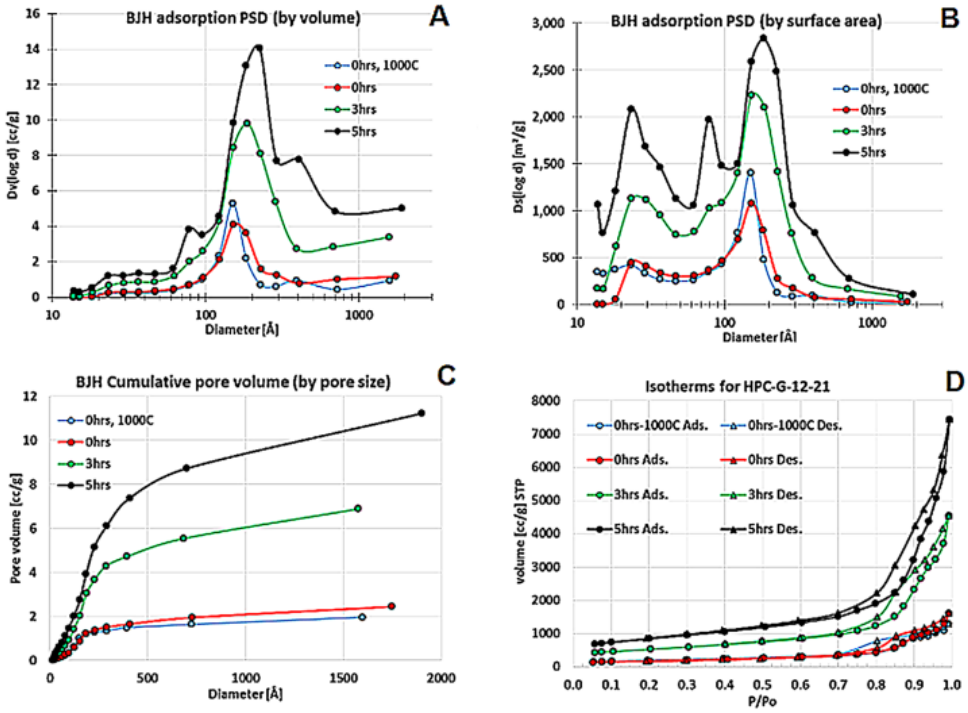

Figure 2. Nitrogen porosimetry data for the HPC-G materials at varying levels of activation showing (a) pore size distribution curves by volume and (b) surface area, as well as (c) cumulative pore volume as a function of pore size; all based on BJH theory. The (d) isotherms for the various levels of activation are also shown.

Conclusions

In summary, a synthesis strategy for a series of tunable hierarchically porous carbons was developed that exhibit a combination of very high surface area (>2500 m^2/g via BET) and large pore volume (>10 cm^3/g via BJH) in one material—a combination which has not been previously accomplished. The incorporation of ice templating was found to play a highly significant role in enhancing these advanced textural characteristics. This synthesis allows for the tunability of not only the porous morphology, but also for the adjustability down to the atomic structure, permitting the same unique textural characteristics in a graphitic/ordered highly porous carbon material. The synthesis strategy presented herein leads to a new direction in the rational design of highly porous graphitic carbon materials.

References

1. Dutta, S.; Bhaumik, A.; Wu, K. C.-W. (2014). Hierarchically Porous Carbon Derived from Polymers and Biomass: Effects of Interconnected Pores in Energy Applications. *Energy Environ. Sci.* 7, 3574-3592

2. Tan, K.W.; Jung, B.; Werner, J. G.; Rhoades, E. R.; Thompson, M. O.; Wiesner, U. (2015). Transient Laser Heating Induced Hierarchical Porous Structures From Block Copolymer–Directed Self-Assembly. *Science* 349, 54-58

3. Hao, P.; Zhao, Z.; Leng, Y.; Tian, J.; Sang, Y.; Boughton, R. I.; Wong, C. P.; Liu, H.; Yang, B. (2015). Graphene-Based Nitrogen Self-Doped Hierarchical Porous Carbon Aerogels Derived from Chitosan for High Performance Supercapacitors. *Nano Energy* 15, 9-23

4. Sahore, R.; Levin, B. D. A.; Pan, M.; Muller, D. A.; DiSalvo, F. J.; Giannelis, E. P. (2016). Design Principles for Optimum Performance of Porous Carbons in Lithium–Sulfur Batteries. *Adv. Energy Mater.* 1600134, 1-9

5. Estevez, L.; Dua, R.; Bhandari, N.; Ramanujapuram, A.; Wang, P.; Giannelis, E. P. (2013). A Facile Approach for the Syntehsis of Monolithic Hierarchical Porous Carbons-High Performance Materials for Amine Based CO_2 Capture and Supercapacitor Electrode. *Energy Environ. Sci.* 6, 1785-1790

6. Deville, S.; Viazzi, C.; Leloup, J.; Lasalle, A.; Guizard, C.; Maire, E.; Adrien, J.; Gremillard, L. (2011). Ice Shaping Properties, Similar to That of Antifreeze Proteins, of a Zirconium Acetate Complex. *PloS One* 6, 1-6

7. Deville, S. (2013). Ice-Templating, Freeze Casting: Beyond Materials Processing. *J. Mater. Res.* 28, 2202-2219

8. Marsh, H.; Reinoso, F. R. (2006). Activated Carbon; Elsevier Science Ltd. Oxford, UK

9. Wang, H.; Yi, H.; Zhu, C.; Wang, X.; Fan, H. J. (2015). Functionalized Highly Porous Graphitic Carbon Fibers for High-Rate Supercapacitive Electrodes. *Nano Energy* 13, 658-669

10. Sun, L.; Tian, C.; Li, M.; Meng, X.; Wang, L.; Wang, R.; Yin, J.; Fu, H. (2013). From Coconut Shell to Porous Graphene-Like Nanosheets for High-Power Supercapacitors. *J. Mater. Chem. A.* 1, 6462-6470

11. Gierszal, K. P.; Jaroniec, M.; Kim, T.-W.; Kim, J.; Ryoo, R. (2008). High Temperature Treatment of Ordered Mesoporous Carbons Prepared by Using Various Carbon Precursors and Ordered Mesoporous Silica Templates. *New J. Chem.* 32, 981-993